Polym. Korea, Vol. 49, No. 4, pp. 464-471 (2025)
https://doi.org/10.7317/pk.2025.49.4.464
ISSN 2234-8077(Online)

다기능성 나노입자를 활용한 폴리우레탄 나노복합재의 침식 저항성 및 제빙 성능 향상

최윤일† · **황은혜**
한국생산기술연구원 목적기반모빌리티그룹 순천뿌리기술지원센터
(2025년 1월 14일 접수, 2025년 3월 14일 수정, 2025년 3월 14일 채택)

Enhancing Erosion Resistance and Deicing Performance of Polyurethane Nanocomposites Using Multifunctional Nanoparticles

Yun-Il Choi† **and Eun-Hye Hwang**
Smart Mobility Materials and Components R&D Group, Korea Institute of Industrial Technology, 34, Haeryongsandan 2-ro, Haeryong-myeon, Suncheon-si, Jeollanam-do 58022, Korea
(Received January 14, 2025; Revised March 14, 2025; Accepted March 14, 2025)

초록: 풍력 터빈 블레이드 리딩 엣지의 침식을 방지하고 제빙 성능을 강화하기 위해 폴리우레탄(PU) 기반 나노복합재를 제작하였다. 이를 위해 carbon nanotube(CNT)/reduced graphene oxide(rGO) 분말 하이브리드 용액에 SiO_2 또는 Al_2O_3 분말을 복합화하여 단일 분말만으로는 달성하기 어려운 기계적·열적 특성을 동시에 개선하고자 하였다. 최적 조건(0.1 wt% SiO_2, 0.05 wt% Al_2O_2)에서 제조된 PU 나노복합재는 순수 PU 대비 연신율이 약 25-35% 향상되었고, 부착 강도는 약 80-100% 증가했으며, 침식 깊이는 약 75-85% 감소하는 우수한 성능을 보였다. 또한, CNT/rGO 분말이 첨가된 PU는 광열 효과가 순수 PU 대비 약 10% 높았고, 0.1 wt% SiO_2 또는 0.05 wt% Al_2O_3를 추가로 첨가하더라도 광열 성능은 CNT/rGO 단일 시스템과 유사한 수준을 유지하였다. 이러한 결과는 다기능성 나노입자를 복합화함으로써 침식 저항성, 기계적 강도, 제빙 성능을 동시에 향상시키는 고성능 PU 나노복합재로서의 잠재력을 보여준다.

Abstract: Polyurethane (PU)-based nanocomposites were developed to protect the leading edge of wind turbine blades from erosion and to enhance de-icing performance. By incorporating a carbon nanotube (CNT)/reduced graphene oxide (rGO) hybrid with SiO_2 and Al_2O_3, mechanical and thermal properties unattainable with single fillers were simultaneously improved. At optimal concentrations (0.1 wt% SiO_2, 0.05 wt% Al_2O_3), the nanocomposites exhibited a 25-35% improvement in tensile elongation, an 80-100% increase in adhesion strength, and a 75-85% reduction in erosion depth compared to pure PU. CNT/rGO also improved photothermal effect by 10% compared to PU under simulated solar radiation. Even with 0.1 wt% SiO_2 or 0.05 wt% Al_2O_3 loading, photothermal effect remained comparable to that of CNT/rGO-only system.

Keywords: polyurethane nanocomposites, carbon nanotube, reduced graphene oxide, silicon oxide, aluminium oxide, erosion resistance, deicing performance.

Introduction

Polyurethane (PU) is widely employed in the wind power industry as a protective coating for the leading edges of turbine blades, shielding them from environmental factors such as rain, hail, and airborne particles that cause erosion and degradation.[1-4] The flexibility and durability of PU coatings effectively extend blade lifespan, reduce maintenance, and help ensure consistent energy production—capabilities increasingly essential as larger turbines operate in extreme conditions.

Despite these advantages, PU coatings remain susceptible to erosion damage, especially at blade leading edges.[1] High-velocity impacts of rain droplets, sand, and other particulates gradually remove the coating, forming irregularities that compromise aerodynamics and lower energy output.[2,3] Erosion-related losses can reduce energy production by up to 20-25%, significantly affecting cost-effectiveness of wind power.[4] This challenge is further magnified in offshore wind farms, where harsher environments—including salt-laden winds, high humidity, and consistent strong winds—accelerate material deterioration.[5] Moreover,

†To whom correspondence should be addressed.
yunil.choi@kitech.re.kr, ORCID 0009-0000-9467-0109

corrosion in marine settings degrades blade structures, and complex offshore maintenance logistics underscore the urgent need for more robust PU coatings.

Recent progress in erosion-resistant coatings for wind turbine blades has focused on PU-based nanocomposites, which combine nanoparticles such as graphene nanoplatelets (GNP), silica-based sol-gel (SiO_2), and cerium oxide (CeO_2).[6-11] Incorporating these nanofillers enhances erosion resistance and wear durability by dispersing stresses and reflecting shock waves from water droplets or solid particles. Hybrid nanocomposites, exemplified by graphene-silica systems, can achieve up to 13 times greater erosion resistance than pure PU, owing to synergistic improvements in hardness and flexibility.[6] Thin-film approaches, particularly sol-gel coatings under 10 μm, further boost performance without adding significant weight—critical for maintaining turbine structural integrity.[9]

In addition to erosion resistance, de-icing has become a critical functionality for modern PU-based nanocomposite coatings.[7,11] Ice build-up can drastically reduce energy output by altering blade aerodynamics and raising rotational loads. Persistent icing not only lowers efficiency but also compromises safety by inducing imbalance and vibration in the rotating blades. Manual or chemical de-icing in offshore installations is often costly, risky, and time-consuming. Hence, integrated de-icing solutions—especially those using conductive nanofillers like CNTs and graphene—offer electrothermal heating for rapid and efficient ice removal.[11] Such capabilities are essential to maintaining stable operation, minimizing downtime, and protecting investments in cold or icing-prone regions.

To further refine and validate these nanocomposites, researchers rely on experimental methods—single impact testing, accelerated erosion testing, numerical simulations—to clarify how variables like impact angle, particle size, and velocity affect wear.[12] Such studies guide the design of coatings fine-tuned for specific operational conditions.[12] The continuing evolution of these materials underscores their potential as sustainable, large-scale solutions for enhancing wind turbine reliability and cost-effectiveness. Addressing the combined challenges of erosion, ice accretion, and marine corrosion is central to improving wind energy productivity, especially as turbines move into more extreme settings.

Building on these advances, we developed high-performance, multifunctional coatings by integrating rGO, CNT, SiO_2, and Al_2O_3 into PU matrices. While prior studies often target single properties—erosion resistance or de-icing—using one or two nanofillers, our research uniquely combines multiple nanomaterials to achieve simultaneous improvements in both erosion durability and anti-/de-icing performance.

Experimental

A PU resin named LEP from JOTUN served as the base material, chosen to address leading edge erosion in wind turbine blades. To develop an electrically conductive PU nanocomposite, a well-dispersed CNT/rGO hybrid liquid (EN Plus, Republic of Korea) was prepared by dissolving 3 wt% CNT, 0.1 wt% rGO, and 0.82 wt% dispersant in N-methyl-2-pyrrolidinone (NMP). This hybrid (1.0 wt%) was then mixed with 99.99%, 20~30 nm SiO_2 or Al_2O_3 nanofillers (MIDAS, OEM product, Republic of Korea) at various concentrations (SiO_2: 0.1, 0.3, 0.5 wt%; Al_2O_3: 0.05, 0.1, 0.3 wt%) (Table 1). The blends were stirred at 150 rpm for 1 h to achieve homogeneous dispersion. Control samples – pure PU and PU with CNT/rGO only – were also prepared. The resulting CNT/rGO-nanofiller mixture was combined with the PU resin and stirred again (150 rpm, 1 h) before adding a hardener. The final mixture was poured into Teflon molds, air-dried for 7 days at room temperature, and formed into solid nanocomposite films (~2 mm thickness) for subsequent testing (Table 2).

The Skyscan 2214 X-ray 3D CT system was used to assess nanoparticle distribution in the PU matrix. Nanocomposite samples were immersed in liquid nitrogen and fractured into smaller

Table 1. Characteristics of CNT/rGO Hybrid Slurry with Additional SiO_2 and Al_2O_3 Nanoparticles for PU Nanocomposite Production

Slurry measurements	Results	
Dispersion medium	NMP (N-methyl-2-pyrrolidone)	
Solid contents (wt%)	CNT	3.0
	rGO	0.1
	SiO_2	0.1, 0.3, 0.5
	Al_2O_3	0.05, 0.1, 0.3
Dispersant	0.82 ± 0.2	

Table 2. Erosion Test Parameters

Erosion test parameters	Values
Nozzle tip diameter (mm)	3
Distance from nozzle to specimen (mm)	5
Flow velocity (m s^{-1})	4.2
Time (h)	3.5
Impingement angle (°)	90
Sand particle size (mm)	0.25 in avg.

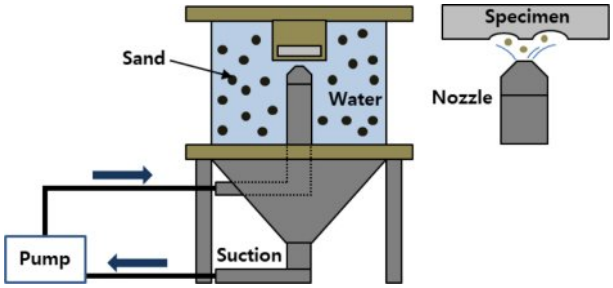

Figure 1. Schematic diagram of the erosion testing apparatus.

pieces for high-resolution CT imaging.

Erosion testing (Figure 1) involved continuously spraying room-temperature water (6 L) containing sand particles (100 g, 0.25 mm average diameter) at 4.2 m/s for 3.5 hours. The nozzle (3 mm diameter) was set 5 mm from the specimen surface with the sand particles recycled through the nozzle to maintain consistent concentration. Each test was repeated three times to ensure reproducibility. Erosion depth was measured via a 3D laser microscope (Keyence VK-X1050) and a digital thickness gauge.

Tensile tests followed KS M ISO 527-1/527-3, using Type 5 dumbbell specimens (thickness ≤1 mm). Specimens measured 75 mm in total length, with a 25 mm gauge length and 4 mm gauge width. Testing proceeded at 200 mm/min and five tests were conducted per sample to verify statistical reliability.

Adhesion strength was evaluated via the ISO 4624 pull-off test. Each PU nanocomposite coating (<100 μm thickness) was applied to an FRP substrate and allowed to fully dry. A dolly was then bonded to the coating and cured for 24 h at room temperature before performing the pull-off test. The maximum tensile force needed to detach the dolly defined the adhesion strength.

Finally, to assess de-icing and anti-icing performance, each specimen was exposed to 1000 W/m² radiant intensity for 780 seconds. Thermocouples (TC) attached to the samples recorded temperature changes throughout the test, indicating how effectively the nanocomposites could heat under simulated sunlight.

Results and Discussion

Nanoparticle Dispersion in PU Nanocomposites. The X-ray 3D CT images in Figure 2 depict the dispersion state of nanoparticles within three PU nanocomposite samples: (a) PU reinforced with 1 wt% CNT/rGO, (b) PU reinforced with 1 wt% CNT/rGO plus an additional 0.1 wt% SiO_2, and (c) PU reinforced with 1 wt% CNT/rGO plus an additional 0.05 wt% Al_2O_3. This

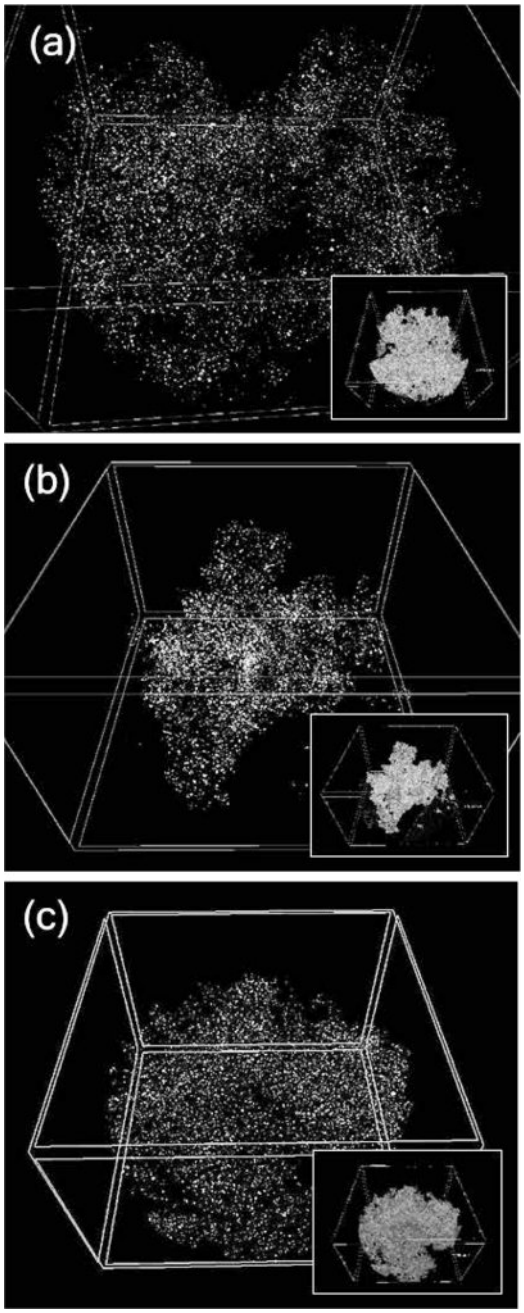

Figure 2. 3D X-ray CT images showing the dispersion of nanoparticles within PU nanocomposites: (a) PU nanocomposite containing CNT/rGO; (b) PU nanocomposite with CNT/rGO and 0.1 wt% SiO_2 nanoparticles; (c) PU nanocomposite with CNT/rGO and 0.05 wt% Al_2O_3 nanoparticles.

non-destructive imaging technique provides three-dimensional information on the distribution of CNT, rGO, SiO_2, and Al_2O_3 in the PU matrix at the macroscale.

It is important to note that X-ray 3D CT has a maximum spatial resolution of approximately 500 nm. While this reso-

lution is sufficient to detect macroscopic features such as large aggregates, it does not fully resolve nanoparticles in the 20-30 nm range including SiO_2 and Al_2O_3. Nonetheless, X-ray 3D CT remains useful for observing whether nanoparticles tend to form large clusters at the bulk level or are relatively well-dispersed throughout the matrix. In the CT images, regions with large clusters of overlapping nanoparticles appear as large white spots.

In Figure 2(a), the CNT/rGO-reinforced PU showed a largely uniform distribution with only minor indications of clustering or voids. Figures 2(b) and 2(c) revealed similar dispersion behavior when 0.1 wt% SiO_2 and 0.05 wt% Al_2O_3 were further introduced, respectively. Although some local regions appeared slightly agglomerated or sparsely populated, the overall nanoparticle dispersion across these samples was still considered homogeneous from a macroscopic standpoint.

Effect of Nanoparticles on Mechanical Properties of PU.

The erosion test results in Figures 3 and 4 demonstrate significant improvements in erosion resistance with the incorporation of nanoparticles into PU. Specifically, the addition of a CNT/rGO hybrid reduced the erosion depth by around 25% from 0.8 to 0.6 mm compared to pure PU with no additives. This improvement is attributed to the reinforcement provided by the CNT/rGO hybrid, which enhances the mechanical properties of PU matrix and makes it more resistant to material loss during erosion. When SiO_2 or Al_2O_3 nanoparticles were added to the CNT/rGO hybrid-reinforced PU, the erosion resistance improved further, with the erosion depth decreasing by approximately 30% at a concentration of 0.1 wt% or 0.05 wt%, respectively.

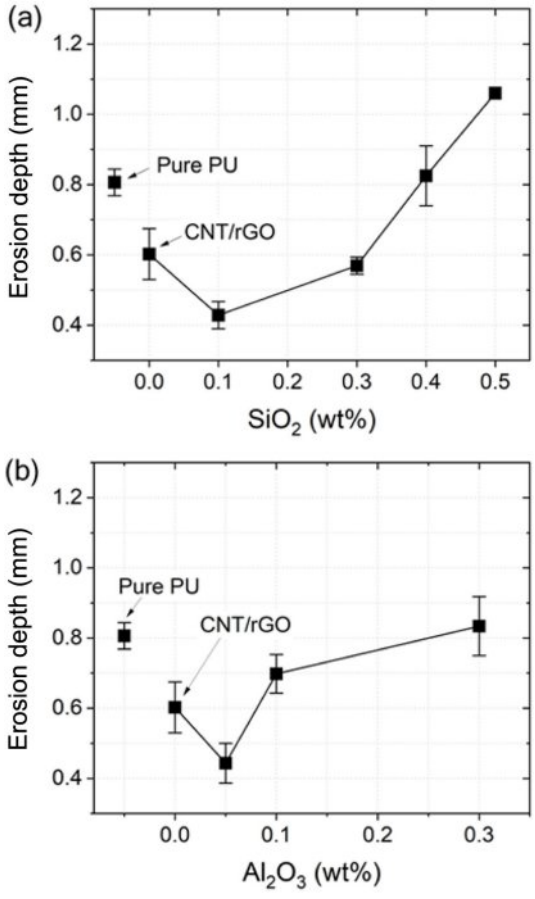

Figure 3. Effects of (a) SiO_2; (b) Al_2O_3 nanoparticles at different concentrations on erosion depth of CNT/rGO-reinforced PU. Erosion test results were carried out using the apparatus shown in Figure 1.

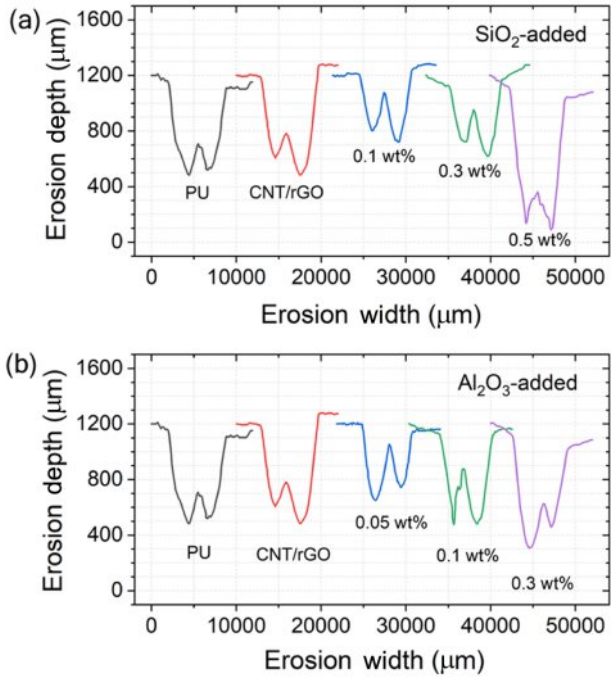

Figure 4. 2D cross-sectional profiles of erosion damage analyzed using 3D laser microscopy after erosion testing for (a) PU nanocomposites with SiO_2 nanoparticles at different concentrations (0.1, 0.3, and 0.5 wt%); (b) PU nanocomposites with Al_2O_3 nanoparticles at different concentrations (0.05, 0.1, and 0.3 wt%).

The incorporation of nanoparticles into PU matrices has been shown to enhance erosion resistance through several key mechanisms.[8,13] The nanoparticles significantly increase the surface hardness of PU composites, making them more resistant to erosive wear. This enhanced hardness acts as a protective barrier, reducing material removal under abrasive conditions. This enhancement in mechanical properties is attributed to the uniform dispersion of nanofillers within the PU matrix, which facilitates effective stress transfer and restricts the mobility of polymer chains, resulting in increased hardness and improved erosion resistance.[13] These results align with our experimental obser-

vations, where the incorporation of SiO_2 or Al_2O_3 nanoparticles into PU matrices led to a significant reduction in erosion depth. The increased surface hardness provided by the nanoparticles likely acts as a protective barrier against abrasive forces, thereby enhancing the erosion resistance of the nanocomposites.

Moreover, nanoparticles are known to improve the ability to dissipate impact energy from abrasive particles effectively. By spreading the stress more evenly throughout the matrix, they minimize localized damage and reduce the likelihood of material degradation. Previous studies have demonstrated that incorporating nanoparticles into polymer matrices enhances the ability to dissipate impact energy from abrasive particles, thereby improving erosion resistance. For instance, research on thermoplastic polyurethane (TPU) nanocomposites reinforced with carbon black (CB) nanoparticles revealed that uniform dispersion of CB significantly improved the tensile strength of the nanocomposites.[14] This enhancement is attributed to the effective stress transfer and energy dissipation facilitated by the interactions between the nanoparticles and polymer chains. Additionally, study on SiO_2 nanoparticle-filled polymer composites have shown that the presence of nanoparticles led to increased energy dissipation during mechanical deformation.[15] Therefore, the SiO_2 nanoparticles contributed to the formation of a reinforced network within the polymer matrix, enhancing its structural integrity and resistance to crack initiation and propagation. These findings align with our experimental observations where the incorporation of SiO_2 and Al_2O_3 nanoparticles into PU matrices resulted in a significant reduction in erosion depth. The improved energy dissipation and reinforced matrix provided by the nanoparticles likely contribute to the enhanced erosion resistance of the PU nanocomposites.

Additionally, the incorporation of nanoparticles also enhanced the elongation properties of the PU nanocomposites, as shown in Figure 5. The addition of 0.05 wt% Al_2O_3 resulted in a peak elongation improvement of approximately 30% compared to the pure PU, while SiO_2 at 0.1 wt% showed a similar elongation enhancement. This improvement is attributed to the ability of nanoparticles to act as stress concentrators that enhance energy dissipation during elongation, while also creating a reinforcing network that prevents premature failure.[16] The increased elongation, in conjunction with improved erosion resistance, indicates that the nanoparticles not only enhance hardness but also contribute to the overall ductility and toughness of the material.

The incorporation of nanoparticles into PU matrices significantly enhanced erosion resistance; however, excessive nanoparticle loading led to a decline in the performance. For the SiO_2 and Al_2O_3-reinforced PU samples, the erosion depth decreased significantly with an optimal concentration of 0.1 wt% and 0.05 wt%, respectively, indicating enhanced erosion resistance at this level. However, when the SiO_2 and Al_2O_3 concentration exceeded 0.1 wt% and 0.05 wt%, respectively, the erosion resistance began to decline. This phenomenon has been widely reported in the literature and can be attributed to multiple factors. Excessive nanoparticle concentrations often result in agglomeration. The agglomerated nanoparticles create stress concentration points within the matrix, weakening the material's ability to withstand impact forces and contributing to crack initiation and propagation.[17] Moreover, the loss of matrix flexibility has been identified as a critical issue. As nanoparticle concentrations increase, the polymer matrix becomes less ductile, leading to reduced toughness and increased brittleness. Previous study demonstrated that excessive carbon black loading in thermoplastic polyurethane composites decreased tensile strength due to reduced polymer chain mobility.[15] This reduced flexibility compromises the ability to absorb and dissipate energy effectively, leading to poorer erosion resistance. Other study reported that graphene nanoparticles enhance mechanical properties when uniformly dispersed; however, at higher concentrations, aggregation negates these benefits by introducing weak zones.[18] This aligns with our observations, where SiO_2 at 0.1 wt% and Al_2O_3 at 0.05 wt% provided the highest erosion resistance. Beyond these concentrations, the erosion resistance decreased likely due to aggregation and the associated issues mentioned above. These findings emphasize the importance of

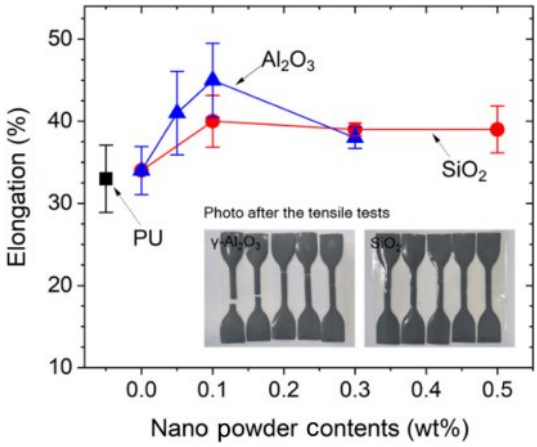

Figure 5. Effects of the Al_2O_3 and SiO_2 nanoparticle concentrations on elongation (%) of PU nanocomposites. Tensile tests were conducted using KS M ISO 527-1/527-3 Type 5 specimens at a test speed of 200 mm/min.

maintaining optimal nanoparticle loading and achieving uniform dispersion within the matrix. Excessive loading not only diminishes the mechanical and erosion-resistant properties but also introduces processing challenges due to increased viscosity and reduced flowability of the composite material.

Enhanced elongation is often associated with improved adhesion strength as materials with higher ductility can better accommodate stresses at the adhesive interface without cracking or debonding. Thus, the uniform dispersion of SiO_2 and Al_2O_3 nanoparticles therefore can reinforce the PU matrix and enhance interfacial bonding. This results in higher adhesion strength compared to the pure PU as shown in Figure 6. The optimal concentration of 0.1 wt% SiO_2 and 0.05 wt% Al_2O_3 nanoparticles improved the adhesion strength of PU nanocomposites to FRP by about 45% (around 4.5 MPa). A continuous increase in adhesion strength with increasing concentration of SiO_2 and Al_2O_3 nanoparticles was observed which differs from the trends in erosion resistance and elongation data. Unlike elongation and erosion resistance, adhesion strength appears less sensitive to the negative effects of nanoparticle agglomeration.

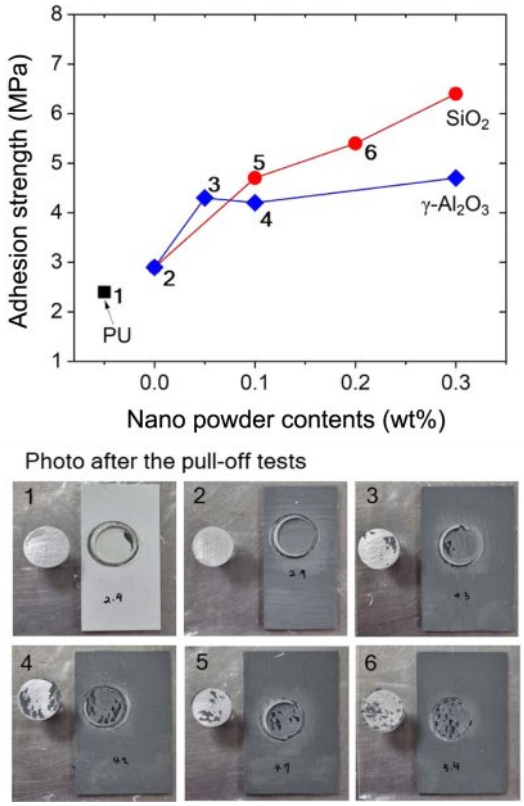

Figure 6. Effects of Al_2O_3 and SiO_2 nanoparticle concentrations on adhesion strength (MPa) of PU nanocomposites. The adhesion strength was measured according to ISO 4624 pull-off tests. The images on the right show the specimens after the pull-off tests.

Even at higher concentrations where some agglomeration may occur the nanoparticles still enhance the interfacial properties. This explains the sustained improvement in adhesion strength which is not significantly compromised by clustering of nanoparticles.

Effect of Nanoparticles on Deicing Performance of PU. When ice forms on the surface of wind turbine blades, rapid ice melting under solar radiation is essential to maintain efficient operation. Figure 7 shows how quickly the developed PU nanocomposites can increase in temperature when exposed to a simulated solar environment, which provides insight into their potential deicing performance in real-world conditions. Specifically, a 1000 W light source was used to simulate solar radiation (Figure 7(a)) and the surface temperature of the nanocomposites was measured over time to determine how effectively they could transfer and distribute heat.

Under these identical solar simulation conditions, the CNT/rGO hybrid PU nanocomposite demonstrated a significant temperature increase, reaching approximately 65 ℃. This rapid heating is primarily attributed to two key properties of CNT and rGO: (1) strong photothermal conversion—they effectively absorb solar radiation and convert it into heat, and (2) high thermal conductivity, which facilitates efficient heat transfer throughout the polyurethane matrix. Once the temperature of a turbine blade surface surpasses 0 ℃, any ice present can begin melting, thereby alleviating issues related to ice build-up.

In contrast, as the concentrations of SiO_2 and Al_2O_3 nanoparticles were increased, the maximum attainable surface temperature showed a decreasing trend. This reduction can be explained by the light-scattering effect of these nanoparticles, which intensifies at higher concentrations and reduces the amount of light absorbed by the PU nanocomposite. In addition, nanoparticle agglomeration at higher loadings can further disrupt thermal pathways, lowering the overall thermal conductivity.

Notably, at the optimal concentrations of SiO_2 (0.1 wt%) and Al_2O_3 (0.05 wt%), the temperature rise was comparable to that of the CNT/rGO-reinforced PU sample, as shown in Figures 7(b) and 7(c). Under 900 s of light exposure, pure PU reached approximately 61 ℃, whereas both the 0.1 wt% SiO_2- and 0.05 wt% Al_2O_3-reinforced PU nanocomposites reached around 65 ℃, which is similar to the CNT/rGO-reinforced composite. This outcome indicates that a balanced system can be achieved by incorporating low loadings of SiO_2 and Al_2O_3—maintaining sufficient thermal conductivity and photothermal efficiency—while minimizing excessive scattering and aggregation.

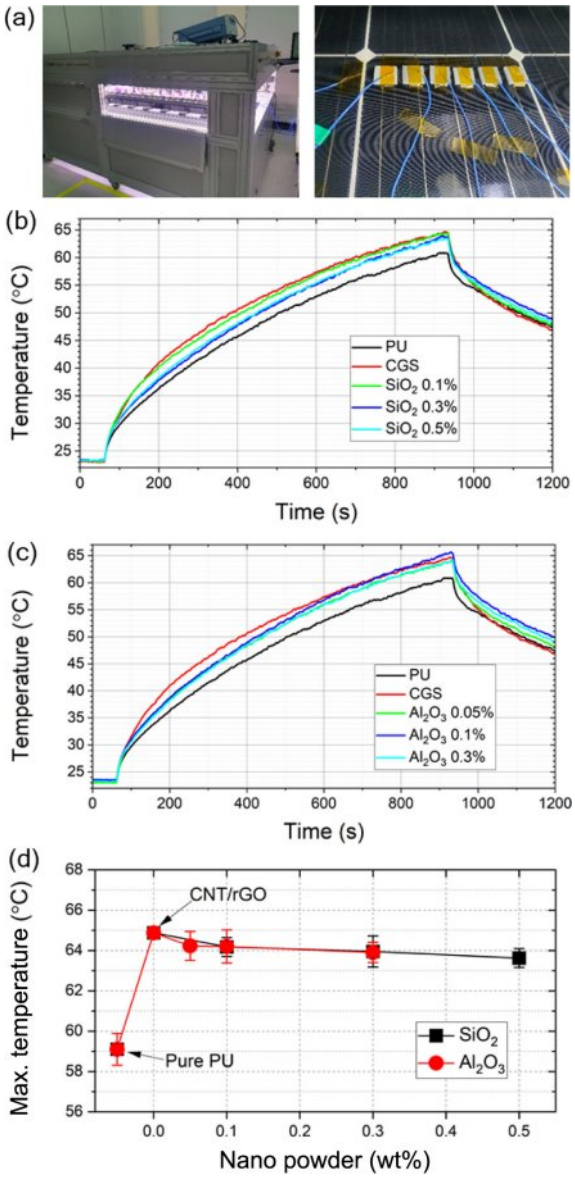

Figure 7. Deicing performance analyzed using a 1000 W light source to simulate solar radiation: (a) Experimental setup for the deicing test showing the sample placement in solar simulator; (b) Temperature profiles of PU nanocomposites with varying SiO_2 nanoparticle concentrations (0.1, 0.3, and 0.5 wt%); (c) Temperature profiles of PU nanocomposites with varying Al_2O_3 nanoparticle concentrations (0.05, 0.1, and 0.3 wt%); (d) Maximum temperature reached as a function of nanoparticle concentration for SiO_2 and Al_2O_3.

Conclusions

This study demonstrates the significant role of nanoparticles in enhancing the mechanical, thermal, and deicing performance of PU nanocomposites, with insights into their dispersion, optimal concentrations, and associated trade-offs. X-ray 3D CT analysis revealed that CNT/rGO, SiO_2, and Al_2O_3 nanoparticles, when properly dispersed, achieve a satisfactory level of uniformity critical for optimizing composite properties. Despite minor clustering observed at nanoscale levels, the overall distribution remained effective in reinforcing the PU matrix. The incorporation of CNT/rGO hybrids significantly enhanced the erosion resistance of PU nanocomposites, reducing material loss by up to 25%. The addition of SiO_2 (0.1 wt%) and Al_2O_3 (0.05 wt%) further improved erosion resistance by up to 30%, attributed to their ability to enhance surface hardness and dissipate impact energy. However, excessive nanoparticle loading resulted in diminished performance due to agglomeration, which introduced stress concentration points and reduced matrix flexibility. This finding underscores the importance of maintaining optimal nanoparticle concentrations and achieving uniform dispersion to maximize mechanical reinforcement. In terms of deicing performance, the CNT/rGO-reinforced PU exhibited superior temperature rise due to its photothermal properties and high thermal conductivity, achieving rapid heating under simulated solar radiation. SiO_2 and Al_2O_3, when added at optimal concentrations, provided comparable thermal performance by balancing light absorption and scattering effects, while maintaining uniform heat transfer pathways. Beyond these concentrations, excessive nanoparticle loading reduced thermal efficiency, highlighting the trade-off between dispersion quality and thermal conductivity. Overall, this study emphasizes the critical balance between nanoparticle concentration, dispersion, and composite performance. The results indicate that CNT/rGO hybrids and optimally loaded SiO_2 and Al_2O_3 nanoparticles significantly enhance PU nanocomposite properties, offering a promising solution for applications in erosion-resistant coatings and rapid deicing systems for wind turbine blades.

Acknowledgments: This work was supported by the National Research Foundation of Korea (NRF) grant funded by the Korea government (MSIT) (2022R1F1A1076146).

Conflict of Interest: The authors declare that there is no conflict of interest.

References

1. Mishnaevsky, L., Jr.; Tempelis, A.; Kuthe, N.; Mahajan, P. Recent Developments in the Protection of Wind Turbine Blades against Leading Edge Erosion: Materials Solutions and Predictive Modelling. *Renewable Energy*, **2023**, 215, 118966.

2. Chen, J.; Wang, J.; Ni, A. A Review on Rain Erosion Protection of Wind Turbine Blades. *J. Coat. Technol. Res.* **2018**, 16, 15-24.
3. Tempelis, A.; Jespersen, K. M.; Dyer, K.; Clack, A.; Mishnaevsky, L. How Leading Edge Roughness Influences Rain Erosion of Wind Turbine Blades? *Wear*, **2024**, 552-553, 205446.
4. Slot, H.; Gelinck, E.; Rentrop, C.; Van Der Heide, E. Leading Edge Erosion of Coated Wind Turbine Blades: Review of Coating Life Models. *Renewable Energy*, **2015**, 80, 837-848.
5. Tumse, S.; Bilgili, M.; Yildirim, A.; Sahin, B. Comparative Analysis of Global Onshore and Offshore Wind Energy Characteristics and Potentials. *Sustainability*, **2024**, 16, 6614.
6. Frost-Jensen Johansen, N.; Mishnaevsky, L.; Dashtkar, A.; Williams, N. A.; Fæster, S.; Silvello, A.; Cano, I. G; Hadavinia, H. Nanoengineered Graphene-Reinforced Coating for Leading Edge Protection of Wind Turbine Blades. *Coatings*, **2021**, 11, 1104.
7. Liang, F.; Gou, J.; Kapat, J.; Gu, H.; Song, G. Multifunctional Nanocomposite Coating for Wind Turbine Blades. *Int. J. Smart Nano Mater.* **2011**, 2, 120-133.
8. Dashtkar, A.; Hadavinia, H.; Sahinkaya, M. N.; Williams, N. A.; Vahid, S.; Ismail, F.; Turner, M. Rain Erosion-Resistant Coatings for Wind Turbine Blades: A Review. *Polym. Polym. Compos.* **2019**, 27, 443-475.
9. Valaker, E. A.; Armada, S.; Wilson, S. Droplet Erosion Protection Coatings for Offshore Wind Turbine Blades. *Energy Procedia*, **2015**, 80, 263-275.
10. Pathak, S. M.; Kumar, V. P.; Bonu, V.; Latha, S.; Mishnaevsky, L.; Lakshmi, R. V.; Bera, P.; Barshilia, H. C. Solid Particle Erosion Studies of Ceramic Oxides Reinforced Water-Based PU Nanocomposite Coatings for Wind Turbine Blade Protection. *Ceram. Int.* **2022**, 48, 35788-35798.
11. Cui, X.; Zhang, N.; Huang, M.; Gao, G.; Liu, S.; Liu, C. Polyurethane-Based Nanocomposite Film with Thermal Deicing Capability and Anti-Erosion for Wind Turbine Blades Protection in Extreme Environments. *J. Mater. Chem. A*, **2023**, 11, 23844-23853.
12. Wang, J.; Gao, J.; Zhang, Y.; Cui, H. Analysis of the Sand Erosion Effect and Wear Mechanism of Wind Turbine Blade Coating. *Energies*, **2024**, 17, 413.
13. Mishnaevsky, L. Toolbox for Optimizing Anti-Erosion Protective Coatings of Wind Turbine Blades: Overview of Mechanisms and Technical Solutions. *Wind Energy*, **2019**, 22, 1636-1653.
14. Dong, M.; Li, Q.; Liu, H.; Liu, C.; Wujcik, E.; Shao, Q.; Ding, T.; Ma, X.; Shen, C.; Guo, Z. Thermoplastic Polyurethane-Carbon Black Nanocomposite Coating: Fabrication and Solid Particle Erosion Resistance. *Polymer*, **2018**, 158, 381-390.
15. Devaprakasam, D. Nanoscale Tribology, Energy Dissipation and Failure Mechanisms of Nano- and Micro-Silica Particle-Filled Polymer Composites. *Tribol. Lett.* **2009**, 34, 11-19.
16. Jin, J.; Song, M.; Yao, K. J.; Chen, L. A Study on Viscoelasticity of Polyurethane–Organoclay Nanocomposites. *J. Appl. Polym. Sci.* **2006**, 99, 3677-3683.
17. Zare, Y.; Rhee, K. Y.; Hui, D. Influences of Nanoparticles Aggregation/Agglomeration on the Interfacial/Interphase and Tensile Properties of Nanocomposites. *Compos. Part B-Eng.* **2017**, 122, 41-46.
18. Wang, X.; Tang, F.; Qi, X.; Lin, Z. Mechanical, Electrochemical, and Durability Behavior of Graphene Nano-Platelet Loaded Epoxy-Resin Composite Coatings. *Compos. Part B-Eng.* **2019**, 176, 107103.